Software Tools for Flexible Control of Radiation Synthesis

Thibaut Carpentier, Olivier Warusfel, Jean-Marc Jot

Software Tools for Flexible Control of Radiation Synthesis

Thibaut Carpentier
STMS Lab, CNRS,
IRCAM, Sorbonne Université
Paris, France
thibaut.carpentier@ircam.fr

Olivier Warusfel
STMS Lab, IRCAM,
CNRS, Sorbonne Université
Paris, France
olivier.warusfel@ircam.fr

Jean-Marc Jot
Virtuel Works LLC
Aptos, CA, USA
jm@virtuelworks.com

***Abstract*—Compact spherical loudspeaker arrays are new tools for the creation of auditory objects in a space. Originally designed for musical and performance purposes – as a substitute for conventional cabinet loudspeakers lacking naturalness in playback – they intent to promote spatial presence and to emulate lifelike directional features of natural sources such as acoustic instruments and performers. They are typically used to reproduce the measured radiation pattern of sound sources, or to steer directional sound beams in order to excite the acoustic environment. The directivity pattern of the sound beams can be adjusted, in orientation and shape, by modal beamforming techniques.**

In electroacoustic music, it is most often desirable to apply dynamic beamforming, i.e. to vary the directional attributes over time, in order to effectively enable a sense of spatial presence or immersion. This paper presents a software tool, intended for creative applications, for the flexible design and intuitive manipulation of spherical beampatterns. In particular, we propose a simple parametric model that allows to synthesize a variety of high-order radiation patterns, and to smoothly transition between shapes. The tool is implemented in the Max environment, making it easy to extend and to interface with remote controllers for interactive applications.

***Index Terms*—directivity pattern, spherical beamforming, loudspeaker arrays, radiation synthesis**

I. Introduction

A well-known limitation of conventional cabinet loudspeakers is that they exhibit a fixed, non-adjustable, radiation pattern, typically with forward-firing drivers. This is especially problematic in the context of mixed music wherein electroacoustic devices and (unamplified) acoustical instrumental sources concurrently operate in the same space. Musical instruments have rich, time-varying, directivity features that interact with the room and affect the temporal and spectral distribution of the perceived sounds. In contrast, common loudspeaker systems tend to be perceived as disembodied, lacking naturalness, and "as if they are operating in entirely different acoustical spaces" [1]. This has motivated the original development of compact (spherical) loudspeaker arrays to achieve freely controllable directivity [2]. Following the pioneering prototype of "La Timée" [3], a number of compact loudspeaker systems have been elaborated, with varying technological specifications (number of transducers, geometrical shape and size, etc.) [4]–[12].

These systems have been used for the reproduction of measured radiation characteristics of sound sources [8], [13]–[16], or more generally to synthesize controlled directivity patterns in a performance context [3], [4], [9], [17]–[24]. These applications have fostered an intense research work, particularly focused on the design of optimal radiation filters [3], [5], [8], [22], [25]–[30], and the perceptual evaluation of the auditory objects produced by compact loudspeaker arrays [31]–[38].

In addition to (re)creating radiation patterns, compact spherical loudspeaker arrays offer the means to project focused beams in arbitrary directions. These sound beams can excite reflective walls, yielding interesting effects in the perceived spatial impression, such as auditory objects that seem more distant than the loudspeaker system. When orchestrated musically, such auditory phenomena are sometimes referred to as sonic sculptures [9], [19]–[23], [38], [39].

The aim of this work is to promote the artistic expressiveness of beamforming with compact loudspeaker arrays, by proposing software tools capable of producing a variety of beampatterns, with simple and flexible user control.

Most compact loudspeaker arrays used nowadays, including the popular IKO [9], relie on a spherical arrangement of transducers. With such spherical geometry, the sound beams can be efficiently designed using modal beamforming techniques. These methods, operating in the spherical harmonics domain, typically allows for independent control of the beam "shape" and direction. They are extensively discussed in the literature, although predominantly applied to (differential) microphone arrays rather than loudspeaker arrays.

Existing works on modal beamforming enable the design of a large class of directivity patterns. However, the design strategies are often motivated by some objective criterion which may not be relevant or user-friendly for artists, composers, or even recording engineers. In this work, we seek to develop models and tools offering smooth, intuitive, and artist-friendly control over a limited number of parameters. Furthermore, it is desired that the models

be simple enough so that time-varying beampatterns can be generated in real-time contexts such as musical performances. Finally, we wish to fully exploit *higher-order* beampatterns, as for instance the IKO is capable of synthesizing 3rd-order Ambisonic features.

In the literature, the most notable similar work is by De Sena and Hacihabiboğlu [40], [41] where the authors proposed a general framework for obtaining a wide range of higher-order beampatterns specified in terms of two (physically relevant) parameters. Their approach encompasses all the conventional directivity patterns such as omnidirectional, sub-cardioid, cardioid, super-cardioid, and hyper-cardioid. However, their method requires the optimization of a convex cost function, which might not be compatible with real-time constraints.

This paper is organized as follows: in section II we review the basics of first-order cardiod patterns; in sections III, IV, and V we present the proposed parametric model for higher-order beampatterns, and examine its pros and cons. Finally, in section VI, we discuss the actual software implementation.

II. First-order "cardioid-like" beampatterns

The family of first-order cardioid-like beampatterns has been well studied in the literature, and extensively used in the fields of recording technique [42]–[47], beamforming [40], [48]–[50], or radiation synthesis [3], [4], [13]. The polar response of first-order cardioid-like beampattern writes

$$\mathcal{Y}(\Theta) = A + (1 - A)\cos\Theta\,, \tag{1}$$

where Θ is the angle between the observed and steered directions, and $A \in \mathbb{R} \cap \big[0\,,\,1\big]$ is an adjustable control parameter. This parametric equation is sometimes referred to as the "Limaçon of Pascal". Other authors [51] also expressed it in the equivalent form

$$\mathcal{Y}(\Theta) = \frac{B}{1+B} + \frac{1}{1+B}\cos\Theta\,, \tag{2}$$

with $B \in \big[0\,,\,\infty\big[$.

With only one degree of freedom (parameter A or B), the cardioid-like parametric model is easy to manipulate, while being able to generate a number of canonical directivity shapes (see Fig. 1), such as

- figure-8 ($A = 0$), also known as bidirectional.
- hyper-cardioid ($A \approx 0.25$), which exhibits the maximum directivity factor (ratio between the response in the look direction and the power-average response across all directions),
- super-cardioid ($A \approx 0.37$), which maximizes the front-to-back ratio (directional gain for signals incident from the front relative to signals incident from the rear). Super-cardioid beamshapes are somewhat similar to the max-r_E beampattern [52], designed so as to optimize the norm of the energy vector.
- cardioid ($A = 0.5$), also referred to as *in-phase* [52], designed to suppress signals impinging from the opposite side ($\Theta = \pm 180°$), while exhibiting a maximally flat response in that direction.
- sub-cardioid ($A \approx 0.7$), sometimes referred to as "forward-oriented omnidirectional".
- omnidirectional ($A = 1$).

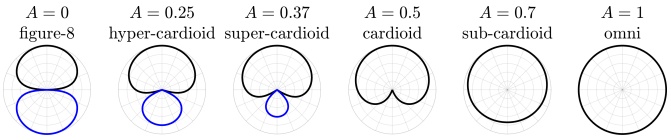

Fig. 1: Polar response of the canonical first-order cardioid-like beampatterns. The radial scale is logarithmic, with 6 dB/division.

III. Higher-order "cardioid-like" beampatterns

A. Axis-symmetric beampatterns

Axis-symmetric spherical beampatterns can be efficiently designed in the spherical harmonics domain [53]–[56]: the frequency-independent beampattern, with finite order N, writes (Eq. (5.24) in [56])

$$\mathcal{Y}_N(\Theta) = \sum_{n=0}^{N} d_{N,n}\,\frac{2n+1}{4\pi}\,\mathcal{P}_n(\cos\Theta)\,, \tag{3}$$

where $\mathcal{P}_n(\cdot)$ is the Legendre polynomial of order n. The $(N+1)$ array weighting factors $d_{N,n}$ are real coefficients which determine the shape of the directivity pattern.

More generally, the Nth-order directional pattern can also be formulated as [41], [49], [57]–[60]

$$\mathcal{Y}_N(\Theta) = \sum_{n=0}^{N} \alpha_{N,n}\,\cos^n\Theta\,. \tag{4}$$

Again, the weights $\alpha_{N,n}$ are a set of real coefficients (different from $d_{N,n}$) that prescribe the directional characteristics of the Nth-order beampattern. They are usually chosen so that the response is normalized to 1 in the look direction ($\Theta = 0$), i.e. $\sum_{n=0}^{N}\alpha_{N,n} = 1$.

The general case of Eq. (4) has been studied in [59], [61]: considering the Legendre polynomials as a special case of the Jacobi polynomials, the authors were able to derive a generic formula to express the weights $d_{N,n}$ as a function of $\alpha_{N,n}$. While this approach is very elegant and allows for a great flexibility in the beampattern design, it requires the choice of $(N+1)$ control parameters, which is not adequate from a user perspective.

B. Target beampattern

In this work, we wish to design a Nth-order cardioid-like beampattern that preserves the simple parametrization of Eq. (1); we propose the following form:

$$\mathcal{Y}_N(\Theta) = \left(A + (1-A)\cos\Theta\right)^N . \tag{5}$$

The restricted class defined by this equation appears as a straightforward generalization of the Limaçon curve (Eq. (1)). Yet, it obviously offers fewer possibilities than the generic formulation in Eq. (4). The major reason for considering this particular class of beampattern is that the algebra becomes simple.

In the following, our aim is to determine the beampattern weights $d_{N,n}$ as a function of the tunable parameter $A \in \mathbb{R} \cap [0\,,\,1]$.

Note that other authors [40], [46], [58] have also suggested a slightly different formulation as $\mathcal{Y}_N(\Theta) = \left(A + (1-A)\cos\Theta\right)\cos^{N-1}(\Theta)$. Although we will focus on Eq. (5) for the remainder of this article, the subsequent discussions could be easily adapted to this alternative form.

C. Case $N = 1$

As a starter, we consider the case of first-order patterns ($N = 1$), for which Eq. (5) writes

$$\mathcal{Y}_1(\Theta) = \left(A + (1-A)\cos\Theta\right) . \tag{6}$$

Alternatively, the first-order beampattern can be expressed by developing Eq. (3)

$$\begin{aligned}\mathcal{Y}_1(\Theta) &= \sum_{n=0}^{n=N=1} d_{1,n}\,\frac{2n+1}{4\pi}\,\mathcal{P}_n(\cos\Theta) \\ &= d_{1,0}\,\frac{1}{4\pi}\,\mathcal{P}_0(\cos\Theta) + d_{1,1}\,\frac{3}{4\pi}\,\mathcal{P}_1(\cos\Theta) \\ &= d_{1,0}\,\frac{1}{4\pi} + d_{1,1}\,\frac{3}{4\pi}\,\cos\Theta\,.\end{aligned} \tag{7}$$

Comparing Eq. (6) and (7), we can straightforwardly identify the weighting coefficients

$$\begin{cases} d_{1,0} &= 4\pi\,A \\ d_{1,1} &= 4\pi\,\frac{1}{3}\,(1-A)\,. \end{cases} \tag{8}$$

This is consistant with well-established results for the family of first-order cardioid patterns [40], [48], [49].

D. Recurrence relation

We now show that the Nth-order coefficients can be obtained by simple recurrence relations. Indeed, the target beampattern in Eq. (5) is such that

$$\begin{aligned}\mathcal{Y}_{N+1}(\Theta) &= \left(A + (1-A)\cos\Theta\right)^{N+1} \\ &= \left(A + (1-A)\cos\Theta\right)\mathcal{Y}_N(\Theta)\,.\end{aligned} \tag{9}$$

According to Eq. (3), this also writes as

$$\mathcal{Y}_{N+1}(\Theta) = \sum_{n=0}^{N+1} d_{N+1,n}\,\frac{2n+1}{4\pi}\,\mathcal{P}_n(\cos\Theta)\,. \tag{10}$$

Now, exploiting Bonnet's recursion formula (see for instance Eq. (3.39) in [60]), valid $\forall n \geq 1$

$$(2n+1)\,x\,\mathcal{P}_n(x) = (n+1)\,\mathcal{P}_{n+1}(x) + n\,\mathcal{P}_{n-1}(x)\,, \tag{11}$$

with $x = \cos\Theta$, it follows

$$\begin{aligned}\mathcal{Y}_{N+1}(\Theta) = A\sum_{n=0}^{N} d_{N,n}\,\frac{2n+1}{4\pi}\,\mathcal{P}_n(\cos\Theta) \\ + (1-A)\sum_{n=0}^{N} d_{N,n}\,\frac{n+1}{4\pi}\,\mathcal{P}_{n+1}(\cos\Theta) \\ + (1-A)\sum_{n=1}^{N} d_{N,n}\,\frac{n}{4\pi}\,\mathcal{P}_{n-1}(\cos\Theta)\,.\end{aligned} \tag{12}$$

Since the Legendre polynomials are orthogonal (see for instance Chapter (3.3) in [60]), we can identify the terms for each $\mathcal{P}_n$, by comparing Eq. (10) and (12). This leads to the following recurrence formula, valid $\forall n,\ 0 < n < N$

$$\begin{aligned}d_{N+1,n} &= A\,d_{N,n} \\ &\quad + (1-A)\,\frac{n}{2n+1}\,d_{N,n-1} \\ &\quad + (1-A)\,\frac{n+1}{2n+1}\,d_{N,n+1}\,,\end{aligned} \tag{13}$$

and the boundary conditions are given by

$$\begin{cases} d_{N+1,0} &= A\,d_{N,0} + (1-A)\,d_{N,1} \\ d_{N+1,N} &= A\,d_{N,N} + (1-A)\,\frac{N}{2N+1}\,d_{N,N-1} \\ d_{N+1,N+1} &= (1-A)\,\frac{N+1}{2N+3}\,d_{N,N}\,. \end{cases} \tag{14}$$

Equations (13) and (14) allow to calculate the weighting coefficients $d_{N,n}$. Results are listed in Table I for $N \leq 4$.

$d_{1,0} = 4\pi\,A$
$d_{1,1} = 4\pi\,\frac{1}{3}\,(1-A)$
$d_{2,0} = 4\pi\left(A^2 + \frac{1}{3}\,(1-A)^2\right)$
$d_{2,1} = 4\pi\,\frac{2}{3}\,A\,(1-A)$
$d_{2,2} = 4\pi\,\frac{2}{15}\,(1-A)^2$
$d_{3,0} = 4\pi\,A\left(A^2 + (1-A)^2\right)$
$d_{3,1} = 4\pi\,\frac{1}{5}\left(-6A^3 + 8A^2 - 3A + 1\right)$
$d_{3,2} = 4\pi\,\frac{6}{15}\,A\,(1-A)^2$
$d_{3,3} = 4\pi\,\frac{6}{105}\,(1-A)^3$
$d_{4,0} = 4\pi\,\frac{1}{5}\left(16A^4 - 24A^3 + 16A^2 - 4A + 1\right)$
$d_{4,1} = 4\pi\,\frac{4}{15}\,A\left(-8A^3 + 14A^2 - 9A + 3\right)$
$d_{4,2} = 4\pi\,\frac{4}{35}\,(1-A)^2\left(8A^2 - 2A + 1\right)$
$d_{4,3} = 4\pi\,\frac{8}{35}\,A\,(1-A)^3$
$d_{4,4} = 4\pi\,\frac{24}{945}\,(1-A)^4$

TABLE I: Beampattern weights for $N \leq 4$.

The polar response of the proposed beampattern is displayed in Fig. 2 for $1 \leq N \leq 5$.

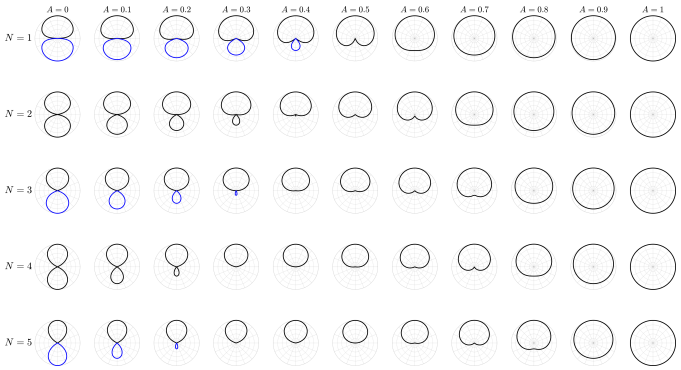

Fig. 2: Cardioid-like beampattern for various values of N and A. The radial scale is logarithmic, with 6 dB/division.

As expected, the resulting polar patterns "look" similar to the canonical shapes (Fig. 1), somehow extended to higher orders. While the solution has the advantage of great simplicity, it also suffers from various limitations that will be discussed in the next section.

IV. Shape Designer

A. Graphical User Interface

We now introduce a graphical user interface (GUI) to control the higher-order cardioid-like beampattern described in the previous section. The directivity function $\mathcal{Y}_N(\Theta)$ (Eq. 5) is fully described by the shape parameter A, and the order N. In Figure 3, we propose a simple 2-D polar interface to "navigate" within the space of realizable shapes. The order N is mapped to the radial coordinate. As a consequence, the center point (origin of the polar grid) corresponds to the omnidirectional pattern ($N = 0$). Instead of mapping directly A to the polar angle, we divide the azimutal plane in five "branches" corresponding to the five canonical directivity shapes (see Fig. 3). This provides a relatively intuitive way to specify the desired beampattern.

Although this work and the proposed GUI are rather intended for artistic usage, it is worth examining certain objective performance measures of the beampatterns produced in each of the five branches.

B. Directivity index – hyper-cardioid branch

The directivity factor quantifies the ratio between the magnitude of the beampattern in the look direction and the power averaged over all directions. For the axis-symmetric beampattern in Eq. (3), the directivity factor writes (see Eq. (5.30) in [56])

$$\mathcal{DF}_N = \frac{\left|\sum_{n=0}^{N} d_{N,n} \frac{2n+1}{4\pi}\right|^2}{\frac{1}{4\pi} \sum_{n=0}^{N} |d_{N,n}|^2 \frac{2n+1}{4\pi}} , \tag{15}$$

and the directivity index is defined such as

$$\mathcal{DI}_N = 10 \log_{10} \mathcal{DF}_N . \tag{16}$$

The directivity index of the higher-order "cardioid-like" beampatterns Eq. (5) is displayed in Figure 4.

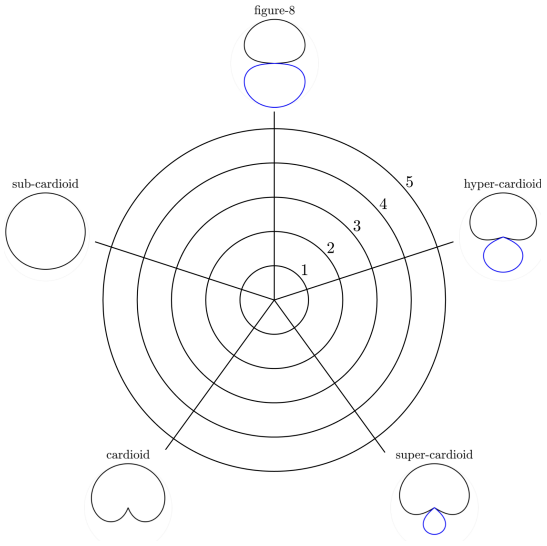

Fig. 3: Proposed GUI for "navigation" within the space of realizable shapes. Here displayed up to order $N = 5$.

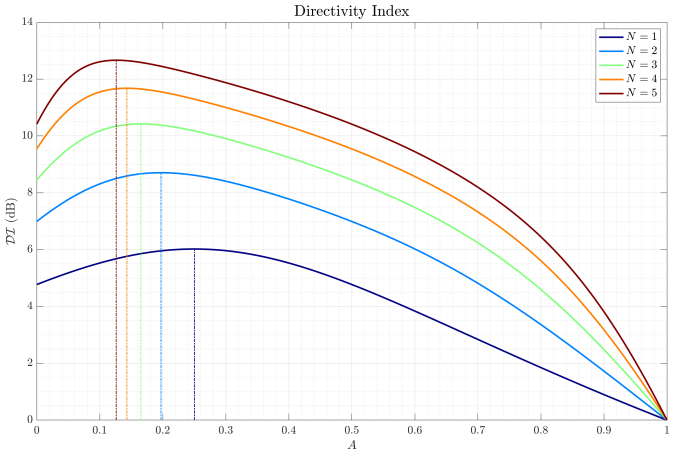

Fig. 4: Directivity index of the "cardioid-like" beampattern, for $1 \leq N \leq 5$. Vertical dashed lines indicate the location of the maximum value for each order.

The observation of this figure reveals two topics of concern. (a) The beampattern does not offer an optimal directivity index. It is known that the highest achievable directivity factor for a Nth-order array is $\mathcal{DF}_N = (N+1)^2$ (see for instance [56], [62]). With Eq. (5), such optimal value is achieved only for $N = 1$. For higher orders, the directivity index of the proposed beampattern is less than optimal. In other words, the proposed method is not able to generate a "true" hyper-cardioid pattern for $N > 1$.

(b) Additionally, the parameter value $A_{\max}$ that maximizes the directivity index depends on the order (see vertical dashed lines in Figure 4): $A_{\max} \approx 0.25$ for $N = 1$; $A_{\max} \approx 0.2$ for $N = 2$; etc. This means that a fixed value of A does not guarantee an actual hyper-cardioid beamshape.

As a consequence, for the hyper-cardioid branch (top-right

in Figure 3), it may be preferable to use an alternative implementation; indeed, the weighting coefficients for Nth-order hyper-cardioid, achieving maximum directivity factor, are known to be [53]–[56] :

$$\forall n \leq N,\ d_{N,n} = \frac{4\pi}{(N+1)^2}\ . \tag{17}$$

C. Front-back ratio – super-cardioid branch

Another important measure for the evaluation of directivity functions is the front-back ratio $\mathcal{F}$, which, as the name suggests, is defined as the ratio between the front and back parts of the beampattern [56], [63]. The front-back ratio according to Eq. (5) is displayed in Figure 5.

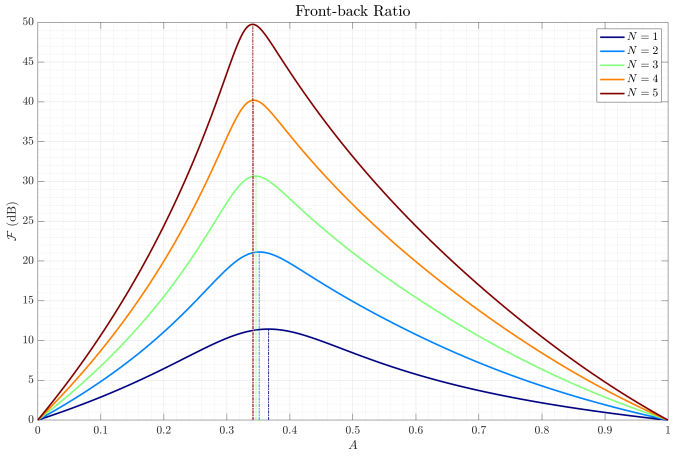

Fig. 5: Front-back ratio of the "cardioid-like" beampattern, for $1 \leq N \leq 5$. Vertical dashed lines indicate the location of the maximum value.

The analysis of this figure raises similar concerns as for the directivity index: the proposed beampattern does not achieve the highest possible front-back ratio (known to be approximately 12, 25, 38, 52, and 66 dB for $N = 1$ to 5 respectively, see [56], [64]) except for $N = 1$, and the parameter value $A_{\max}$ that maximizes $\mathcal{F}$ varies with the order N. In other words, the proposed beampattern (with $A \approx 0.37$) does not realize an actual super-cardioid beamshape for higher orders.

So again, it might be preferable to replace the super-cardioid branch (bottom-right in Figure 3) with the known optimal solution for maximum front-back ratio, the derivation of which can be found in [49] or Chapter 6.5 in [56].

D. In-phase criterion – cardioid branch

The cardioid branch (bottom-left in Figure 3) is expected to exhibit a null in direction $\Theta = \pm 180°$ while ensuring maximal flatness in that direction, i.e.

$$\left.\frac{\partial^n \mathcal{Y}_N(\Theta)}{\partial \Theta^n}\right|_{\Theta=\pm 180°} = 0 \ \text{ for } \ n = 1, ..., N-1\ . \tag{18}$$

Considering $A = 0.5$, the cardioid-like beampattern in Eq. (5) reduces to

$$\mathcal{Y}_N(\Theta) = \left(\frac{1+\cos\Theta}{2}\right)^N\ , \tag{19}$$

and it is straightforward to see that this is a solution to the maximal flatness problem Eq. (18). Alternatively, one can also observe that introducing $A = 0.5$ into Equations (13) and (14) leads to

$$\forall n \leq N,\ d_{N,n} = 4\pi\,\frac{(N!)^2}{(N+n+1)!\,(N-n)!}\ , \tag{20}$$

which is consistent with the well-known *in-phase* formulae (see Eq. (A.75) in [52] or Eq. (12) in [65]).

We conclude that $A = 0.5$ indeed generates an optimal Nth-order cardioid beampattern.

E. Sub-cardioid branch

To the best of the authors' knowledge, there is no clearly established criterion for the design of sub-cardioid beampatterns, besides exhibiting a relatively smooth attenuation in the rear. It is clear that a fixed value of $A \approx 0.7$ cannot be an optimal choice for arbitrary orders N; nevertheless, for the sake of simplicity, we will assume that this is acceptable for relatively low orders.

F. Summary

In this section, we have seen that, for each of the five canonical branches of the GUI proposed in Figure 3, it is possible to derive analytically the weighting factors $d_{N,n}$. Although Eq. (5) is quite generic and simple, it does not allow for optimal hyper-cardioid and super-cardioid designs. For the remainder of this article, these two branches will be implemented with the optimal solutions as presented in Equations (17) and (20).

V. Interpolation between patterns

In order to offer flexible control, the design space proposed in Figure 3 should be fully and continuously browsable. This requires smooth control along the radial axis (i.e. the design order N) and the azimutal direction (i.e. the design criterion w.r.t. the five canonical shapes).

A. Interpolation between orders

The beampattern design strategies discussed in the previous sections are only available for integer orders $N \in \mathbb{N}$. To achieve continuous control along the radial axis, we need to design beampatterns for fractional orders $\nu \in \mathbb{R}$. A simple way to do so is by interpolating between two adjacent integer orders: considering the fractional order $\nu \in \mathbb{R} \cap \left[(N-1)\,, N\right[$, $\mathcal{Y}_\nu(\Theta)$ is constructed by interpolation between beampatterns of order $N-1$ and N :

$$\mathcal{Y}_\nu(\Theta) = \alpha\,\mathcal{Y}_N(\Theta) + (1-\alpha)\,\mathcal{Y}_{N-1}(\Theta)\ , \tag{21}$$

where $\alpha \in \left[0\,, 1\right]$ is an interpolation factor to be determined.

It is tempting to extend the higher-order cardioid-like beampattern in Eq. (5) to fractional orders $\nu \in \mathbb{R}$ as

$$\mathcal{Y}_\nu(\Theta) = \left(A + (1-A)\cos\Theta\right)^\nu . \tag{22}$$

The latter is valid only in the restricted domain $A \in \left[\frac{1}{2}, 1\right[$, wherein it is easy to solve Eq. (21), leading to the solution:

$$\alpha = \frac{A^{\nu-N+1} - 1}{A - 1} . \tag{23}$$

However, the domain where $A \in \left[0, \frac{1}{2}\right[$ is more problematic.

Alternative approaches to the design of fractional-order beampatterns have also been discussed in the literature, with proposals to determine the optimal interpolation factor α to meet specific design criteria. [66], [67] have addressed the design of 2D (horizontal-only) beampatterns; 3D fractional-order hyper-cardioid patterns have been examined in [68], and the approach was later generalized to other shapes (such as super-cardioid, max-r_E, etc.) in [64].

While these approaches are elegant and optimal in some sense, they are not easily generalizable to arbitrary beam shapes (e.g. figure-8). In this work, we have therefore adopted a much simpler strategy, with a straightforward linear interpolation between patterns of order $N-1$ and N, i.e. we choose the following interpolation factor : $\alpha = \nu - (N-1)$.

B. Interpolation between branches

Similarly, interpolation between branches, i.e. along the azimutal direction and for a fixed radius/order ν, is simply and naively implemented by linear interpolation between the two adjacent branches. Although such implementation does not ensure linear variation of the beampattern characteristics (directivity index, front-back ratio, etc), this is considered acceptable at least for artistic usages.

C. Results

We now present some results for our final implementation, which includes the five canonical branches as detailed in section IV, and the interpolation procedure described above (section V). Figure 6 displays the directivity index of the produced beampattern, up to order $N = 5$; it obviously exhibits maximum values for the hyper-cardioid branch, and for higher orders (increasing values of ν). Figure 7 shows the front-back ratio which, as expected, is optimal in the super-cardioid branch. Additionally, in Figure 8 we present the beamwidth at -6 dB, i.e. the angular width of the main lobe, at 6 dB below its peak. We speculate that the beamwidth might be a significant criterion to consider when projecting sound beams.

These figures reveal that the proposed interface is able to generate a relatively wide range of contrasting radiation patterns, with relatively smooth transitions when browsing through the polar grid.

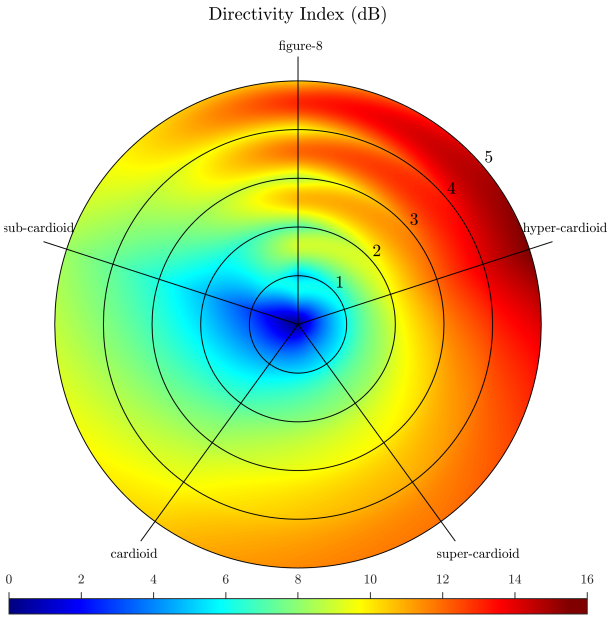

Fig. 6: Directivity Index (in dB). Up to order $N = 5$.

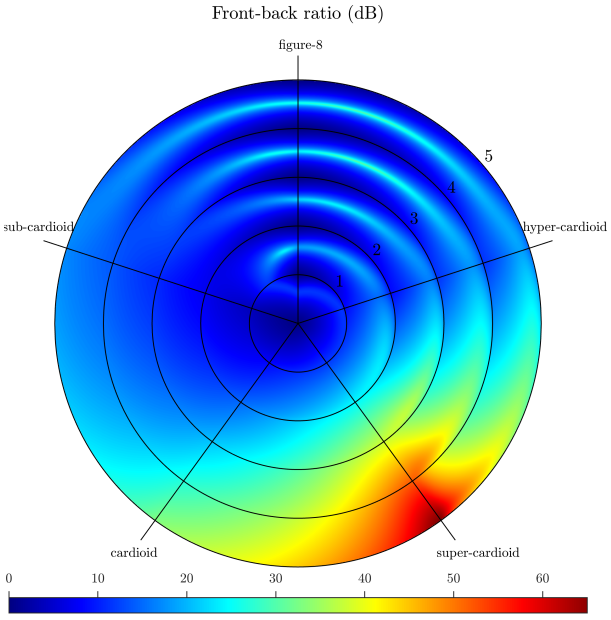

Fig. 7: Front-back ratio. Up to order $N = 5$.

VI. Software Implementation

The technique presented in the previous sections, as well as the corresponding GUI, have been implemented in the Cycling'74 Max environment, as part of the Ircam Spat toolbox [69]. The main control panel is displayed in Figure 9.

It is divided in three main modules, from top to bottom: (a) first, an incoming monophonic signal goes through a filterbank, so that the radiation pattern is controllable in several frequency bands. By default, a 3-band Linkwitz–Riley

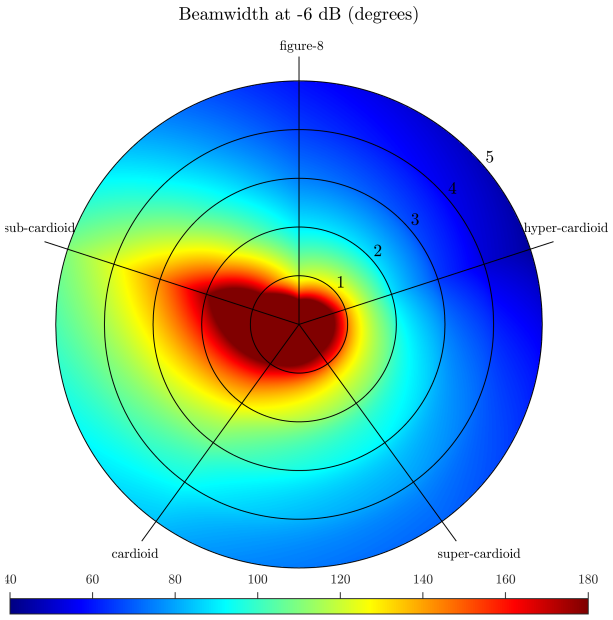

Fig. 8: Beamwidth. Up to order $N = 5$.

crossover filter [70] (having a flat amplitude response with a smoothly changing phase response) is used. The crossover frequencies can be adjusted, and the corresponding low/mid/high bands are depicted in red, green, and blue color respectively. The choice of three frequency bands is a compromise between complexity and perceptual relevance. Yet, the module can be straightforwardly extended to a higher number of frequency bands, if necessary. (b) The second module is the "shape designer", implementing the concept presented in Figure 3. It allows to specify the beampattern characteristics, for each frequency band (depicted by the small dots with corresponding color code). (c) Finally, a steering unit is used to adjust the orientation (azimuth and elevation) of the radiation patterns. The signals are encoded into Nth-order Ambisonic by applying the spherical harmonic weight coefficients, as detailed in the previous paragraphs. Finally, the three Ambisonic-encoded frequency bands are recombined for subsequent decoding (i.e. typically for diffusion with a spherical loudspeaker array).

It should be noted that two adjacent bands overlap near the crossover frequencies; therefore the radiation pattern actually synthesized in that frequency region will be a mix of the corresponding theoretical beampatterns (as they are depicted in bottom of Figure 9).

It is also worth noting that the steering unit allows for independent control of the beam orientation in each frequency band: in the example presented in Figure 9(c), the direction axes are substantially different in the three frequency bands. This feature may be useful to simulate the radiation characteristics of certain instruments, such as woodwinds, that may radiate sound in significantly different directions depending on frequency [71]–[74].

All the control parameters of the UI can be equivalently

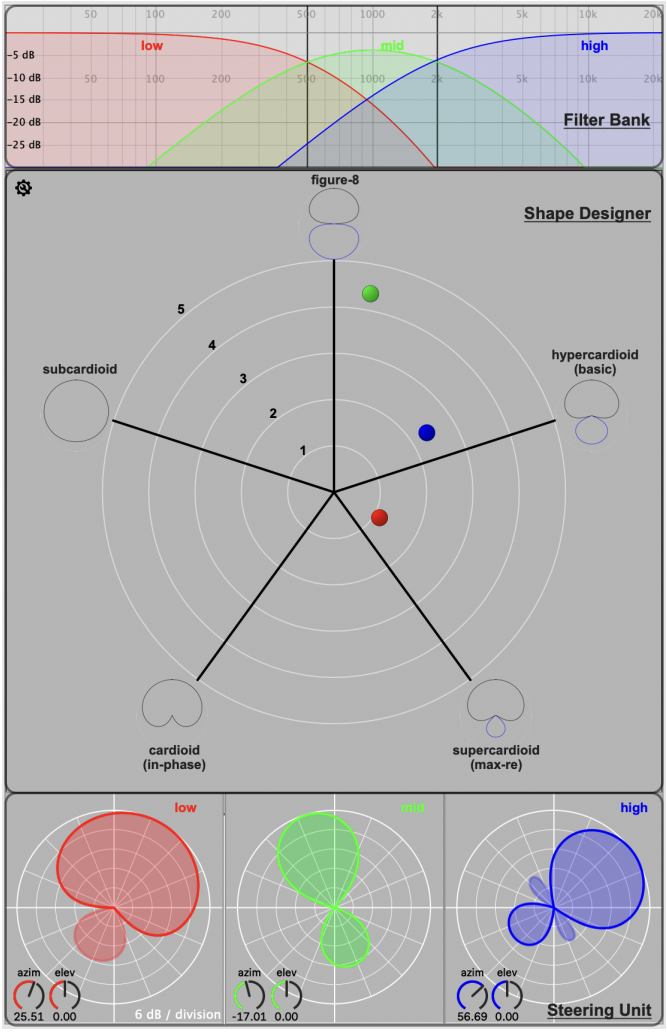

Fig. 9: GUI for the radiation shape designer (here presented for $N = 5$). (a) Top: 3-band filter bank. (b) Middle: directivity shape designer. (c) Bottom: directivity steering unit.

adjusted with the mouse, via conventional Max messages, or over OSC [75]. OSC messages are especially interesting as they allow for time-varying automation and remote control of the parameters. Creating time-variant radiation effects is known to be particularly effective in spatial electroacoustic music [1], [22], [23], as this allows to emulate lifelike directional features of natural sources such as acoustic instruments and performers.

Being integrated in the Max environment, the tool can be easily extended, modified, or combined with other packages, in order to meet the particular needs of each user.

VII. Conclusion

In this article, we have presented an analytical method to design higher-order cardioid-like beampatterns, adjustable with a single "shape" parameter A (Eq. 5). We showed that this model has some limitations that can be overcome if precise

design criteria (maximum directivity index, front-back ratio, etc.) are expected. We have then proposed a simple GUI that combines different design strategies in a unified interface, allowing for the flexible and intuitive manipulation of cardioid-like directivity patterns. The tool is typically intended for the control of radiation synthesis with spherical loudspeaker arrays. Yet, the relevance and usefulness of the proposed tool for artistic uses remain to be evaluated in actual productions, and future work will assess user experience (UX). In any case, the prototype is designed in a quite open and modular way, in order to evolve agilely based on the users' feedback.

References

[1] D. Wessel, "Instruments That Learn, Refined Controllers, and Source Model Loudspeakers," *Computer Music Journal*, vol. 15, no. 4, pp. 82 – 86, Winter 1991. https://doi.org/10.2307/3681079

[2] R. Caussé, J.-F. Bresciani, and O. Warusfel, "Radiation of Musical Instruments and Control of Reproduction with Loudspeakers," in *Proc. of the International Symposium of Music Acoustics (ISMA)*, Tokyo, Japan, August 1992, pp. 67 – 70.

[3] O. Warusfel, P. Derogis, and R. Caussé, "Radiation Synthesis with Digitally Controlled Loudspeakers," in *Proc. of the 103rd Convention of the Audio Engineering Society (AES)*, New York, NY, USA, Sept 1997. http://www.aes.org/e-lib/browse.cfm?elib=7202

[4] O. Warusfel and N. Misdariis, "Directivity synthesis with 3D array of loudspeakers : application for stage performance," in *Proc. of the International Conference on Digital Audio Effects (DAFX-01)*, Limerick, Ireland, December 2001.

[5] R. Avizienis, A. Freed, P. Kassakian, and D. Wessel, "A Compact 120 Independent Element Spherical Loudspeaker Array with Programable Radiation Patterns," in *Proc. of the 120th Convention of the Audio Engineering Society (AES)*, Paris, France, May 2006. http://www.aes.org/e-lib/browse.cfm?elib=13587

[6] D. Lock, G. Schiemer, and L. Ong, "Orbophone: a new interface for radiating sound and image," in *Proc. of the 12th International Conference on Auditory Display (ICAD)*, London, UK, June 2006.

[7] M. Pollow, "Variable directivity of dodecahedron loudspeakers," Master's thesis, RWTH University, Aachen, Germany, December 2007.

[8] F. Zotter, "Analysis and Synthesis of Sound-Radiation with Spherical Arrays," Ph.D. dissertation, IEM Institute of Electronic Music and Acoustics University of Music and Performing Arts, Graz, Austria, 2009.

[9] F. Zotter, M. Zaunschirm, M. Frank, and M. Kronlachner, "A Beamformer to Play with Wall Reflections: The Icosahedral Loudspeaker," *Computer Music Journal*, vol. 41, no. 3, pp. 50 – 68, Fall 2017. https://doi.org/10.1162/comj_a_00429

[10] P. R. Cook and D. Trueman, "NBody: Interactive Multidirectional Musical Instrument Body Radiation Simulators, and a Database of Measured Impulse Responses," in *Proc. of the International Computer Music Conference (ICMC)*, Ann Arbor, MI, USA, October 1998.

[11] D. Trueman, C. Bahn, and P. R. Cook, "Alternative Voices for Electronic Sound: Spherical Speakers and Sensor-Speaker Arrays (SenSAs)," in *Proc. of the International Computer Music Conference (ICMC)*, Berlin, Germany, August 2000.

[12] D. Trueman and P. R. Cook, "BoSSA: The Deconstructed Violin Reconstructed," *Journal of New Music Research*, vol. 29, no. 2, pp. 121 – 130, 2000. https://doi.org/10.1076/jnmr.29.2.121.3098

[13] N. Misdariis, F. Nicolas, O. Warusfel, and R. Caussé, "Radiation Control on Multi-Loudspeaker Device : La Timée," in *Proc. of the International Computer Music Conference (ICMC)*, Havana, Cuba, 2001.

[14] F. Zotter, H. Pomberger, and A. Schmeder, "Efficient directivity pattern control for spherical loudspeaker arrays," in *Proc. of Acoustics 2008*, Paris, France, July 2008. https://doi.org/10.1121/1.2934914

[15] M. Pollow and G. K. Behler, "Variable Directivity for Platonic Sound Sources Based on Spherical Harmonics Optimization," *Acta Acustica united with Acustica*, vol. 95, pp. 1082 – 1092, 2009. https://doi.org/10.3813/AAA.918240

[16] M. Noisternig, F. Zotter, and B. F. G. Katz, "Reconstructing sound source directivity in virtual acoustic environments," in *Principles and Applications of Spatial Hearing*, Y. Suzuki, D. Brungart, and H. Kato, Eds. World Scientific Press, 2011, pp. 357 – 373. https://doi.org/10.1142/7674

[17] O. Warusfel and N. Misdariis, "Sound Source Radiation Synthesis : from Stage Performance to Domestic Rendering," in *Proc. of the 116th Convention of the Audio Engineering Society (AES)*, Berlin, Germany, May 2004. http://www.aes.org/e-lib/browse.cfm?elib=12793

[18] A. Schmeder, "An exploration of design parameters for human-interactive systems with compact spherical loudspeaker arrays," in *Proc. of the 1st Ambisonics Symposium*, Graz, Austria, June 2009.

[19] G. K. Sharma, F. Zotter, and M. Frank, "Orchestrating wall reflections in space by icosahedral loudspeaker: findings from first artistic research exploration," in *Proc. of the International Computer Music Conference (ICMC) / Sound and Music Computing (SMC)*, Athens, Greece, September 2014.

[20] M. Frank, G. K. Sharma, and F. Zotter, "What we already know about spatialization with compact spherical arrays as variable-directivity loudspeakers," in *Proc. of inSONIC2015, Aesthetics of Spatial Audio in Sound, Music and Sound Art*, Karlsruhe, Germany, November 2015.

[21] G. K. Sharma, "Composing with Sculptural Sound Phenomena in Computer Music," Ph.D. dissertation, University of Music and Performing Arts, Graz, Austria, September 2016.

[22] F. Wendt, G. K. Sharma, M. Frank, F. Zotter, and R. Höldrich, "Perception of Spatial Sound Phenomena Created by the Icosahedral Loudspeaker," *Computer Music Journal*, vol. 41, no. 1, pp. 76 – 88, 2017. https://doi.org/10.1162/COMJ_a_00396

[23] G. K. Sharma, M. Frank, and F. Zotter, "Evaluation of Three Auditory-Sculptural Qualities Created by an Icosahedral Loudspeaker," *Applied Sciences*, vol. 9, pp. 1 – 16, 2019. https://doi.org/10.3390/app9132698

[24] A. Einbond, J. Bresson, D. Schwarz, and T. Carpentier, "Instrumental Radiation Patterns as Models for Corpus-Based Spatial Sound Synthesis: *Cosmologies* for Piano and 3D Electronics," in *Proc. of the 47th International Computer Music Conference (ICMC)*, Santiago, Chile, July 2021, pp. 148 – 153.

[25] P. Kassakian and D. Wessel, "Design of Low-Order Filters for Radiation Synthesis," in *Proc. of the 115th Convention of the Audio Engineering Society (AES)*, New York, NY, USA, October 2003. http://www.aes.org/e-lib/browse.cfm?elib=12448

[26] ——, "Characterization of Spherical Loudspeaker Arrays," in *Proc. of the 117th Convention of the Audio Engineering Society (AES)*, San Francisco, CA, USA, October 2004. http://www.aes.org/e-lib/browse.cfm?elib=12940

[27] P. Kassakian, "Magnitude Least-Squares Fitting via Semidefinite Programming with Applications to Beamforming and Multidimensional Filter Design," in *Proc. of the IEEE International Conference on Acoustics, Speech and Signal Processing (ICASSP)*, Philadelphia, PA, USA, March 2005. https://doi.org/10.1109/ICASSP.2005.1415644

[28] F. Zotter and R. Höldrich, "Modeling Radiation Synthesis with Spherical Loudspeaker Arrays," in *Proc. of the 19th International Congress on Acoustics*, Madrid, Spain, September 2007.

[29] F. Zotter and M. Frank, *Ambisonics: A Practical 3D Audio Theory for Recording, Studio Production, Sound Reinforcement, and Virtual Reality*, 1st ed. Springer, 2019. https://doi.org/10.1007/978-3-030-17207-7

[30] B. Rafaely and D. Khaykin, "Optimal Model-Based Beamforming and Independent Steering for Spherical Loudspeaker Arrays," *IEEE Transactions on Acoustics, Speech, and Signal Processing*, vol. 19, no. 7, pp. 2234 – 2238, September 2011. https://doi.org/10.1109/tasl.2011.2116011

[31] T. Wühle, S. Merchel, and M. E. Altinsoy, "The Precedence Effect in Scenarios with Projected Sound," *Journal of the Audio Engineering Society*, vol. 67, no. 3, pp. 92 – 100, March 2019. https://doi.org/10.17743/jaes.2018.0074

[32] F. Zotter and M. Frank, "Investigation of Auditory Objects Caused by Directional Sound Sources in Rooms," *Acta Physica Polonica*, vol. 128, pp. A–1 – A–10, 2015. https://doi.org/10.12693/aphyspola.128.a-5

[33] M. Zaunschirm, M. Frank, and F. Zotter, "An Interactive Virtual Icosahedral Loudspeaker Array," in *Proc. of the DAGA*, Aachen, Germany, March 2016.

[34] F. Zotter, M. Frank, A. Fuchs, and D. Rudrich, "Preliminary study on the perception of orientation-changing directional sound sources in rooms," in *Proc. of the Forum Acusticum*, Kraków, Poland, September 2014.

[35] F. Wendt, M. Frank, F. Zotter, and R. Höldrich, "Directivity Patterns Controlling the Auditory Source Distance," in *Proc. of the 19th International Conference on Digital Audio Effects (DAFx-16)*, Brno, Czech Republic, September 2016, pp. 295 – 300.

[36] F. Wendt, F. Zotter, M. Frank, and R. Höldrich, "Auditory Distance Control Using a Variable-Directivity Loudspeaker," *Applied Sciences*, vol. 7, no. 7, 2017. https://doi.org/10.3390/app7070666

[37] F. Zagala, J. Linke, F. Zotter, and M. Frank, "Amplitude Panning between Beamforming-Controlled Direct and Reflected Sound," in *Proc. of the 142nd Convention of the Audio Engineering Society (AES)*, Berlin, Germany, May 2017. http://www.aes.org/e-lib/browse.cfm?elib=18679

[38] F. Zotter, "Virtual Acoustics under Variable Ambisonic Perspectives," IEM institut für elektronische musik und akustik, Graz, Austria, Habilitation Thesis, May 2022.

[39] G. K. Sharma, M. Frank, and F. Zotter, "Towards Understanding and Verbalizing Spatial Sound Phenomena in Electronic Music," in *Proc. of inSONIC2015, Aesthetics of Spatial Audio in Sound, Music and Sound Art*, Karlsruhe, Germany, November 2015.

[40] E. De Sena, H. Hacihabiboglu, and Z. Cvetkovic, "On the Design and Implementation of Higher Order Differential Microphones," *IEEE Transactions on Audio, Speech, and Language Processing*, vol. 20, no. 1, pp. 162 – 174, June 2012. https://doi.org/10.1109/TASL.2011.2159204

[41] E. D. Sena, H. Hachabiboglu, and Z. Cvetkovic, "A generalized design method for directivity patterns of spherical microphone arrays," in *Proc. of the IEEE International Conference on Acoustics, Speech and Signal Processing (ICASSP)*, Prague, Czech Republic, May 2011, pp. 125 – 128. https://doi.org/10.1109/ICASSP.2011.5946344

[42] R. N. Marshall and W. R. Harry, "A New Microphone Providing Uniform Directivity over an Extended Frequency Range," *Journal of the Acoustical Society of America*, vol. 12, no. 4, pp. 481 – 498, April 1941. https://doi.org/10.1121/1.1916128

[43] H. F. Olson, "Polydirectional Microphone," *Proceedings of the IRE*, vol. 32, no. 2, pp. 77–82, February 1944. https://doi.org/10.1109/JRPROC.1944.229734

[44] H. F. Olson, J. Preston, and J. Bleazey, "The uniaxial microphone," *Transactions of the IRE Professional Group on Audio*, vol. AU-1, no. 4, pp. 12 – 19, July/August 1953. https://doi.org/10.1109/T-SP.1953.28141

[45] H. F. Olson, "Directional Microphones," *Journal of the Audio Engineering Society*, vol. 15, no. 4, pp. 420 – 430, October 1967. http://www.aes.org/e-lib/browse.cfm?elib=1073

[46] J. Eargle, *Handbook of Recording Engineering – fourth edition*. Springer, 2006. https://doi.org/10.1007/0-387-28471-0

[47] E. Pfanzagl-Cardone, *The Art and Science of Surround and Stereo Recording – Including 3D Audio Techniques*, 1st ed. Springer, 2020. https://doi.org/10.1007/978-3-7091-4891-4

[48] G. W. Elko and A.-T. N. Pong, "A steerable and variable first-order differential microphone array," in *Proc. of the IEEE International Conference on Acoustics, Speech and Signal Processing (ICASSP)*, vol. 1, Munich, Germany, April 1997, pp. 223 – 226. https://doi.org/10.1109/ICASSP.1997.599609

[49] G. W. Elko, "Superdirectional microphone arrays," in *Acoustic Signal Processing for Telecommunication*, S. L. Gay and J. Benesty, Eds. Springer, 2000, pp. 181 – 237. https://doi.org/10.1007/978-1-4419-8644-3_10

[50] J. Merimaa, "Applications of a 3-D Microphone Array," in *Proc. of the 112th Convention of the Audio Engineering Society (AES)*, Munich, Germany, May 2002. http://www.aes.org/e-lib/browse.cfm?elib=11337

[51] X. Zhao, J. Benesty, G. Huang, and J. Chen, "On a Particular Family of Differential Beamformers With Cardioid-Like and No-Null Patterns," *IEEE Signal Processing Letters*, vol. 28, pp. 140 – 144, 2021. https://doi.org/10.1109/LSP.2020.3047721

[52] J. Daniel, "Représentation de champs acoustiques, application à la transmission et à la reproduction de scènes sonores complexes dans un contexte multimédia," Ph.D. dissertation, Université de Paris VI, 2001.

[53] J. Meyer and G. Elko, "A highly scalable spherical microphone array based on an orthonormal decomposition of the soundfield," in *Proc. of the IEEE International Conference on Acoustics, Speech and Signal Processing (ICASSP)*, vol. 2. Orlando, FL, USA: IEEE, May 2002, pp. II–1781–II–1784. http://dx.doi.org/10.1109/ICASSP.2002.5744968

[54] J. Meyer and G. W. Elko, "Spherical microphone arrays for 3d sound recording," in *Audio Signal Processing for Next-Generation Multimedia Communication Systems*, Y. Huang and J. Benesty, Eds. Kluwer, 2004, ch. 3, pp. 67 – 89. https://doi.org/10.1007/1-4020-7769-6_3

[55] D. P. Jarrett, E. A. P. Habets, and P. A. Naylor, *Theory and Applications of Spherical Microphone Array Processing*. Springer-Verlag, 2017. https://doi.org/10.1007/978-3-319-42211-4

[56] B. Rafaely, *Fundamentals of Spherical Array Processing*, 2nd ed. Springer-Verlag, 2019. https://doi.org/10.1007/978-3-319-99561-8

[57] T. D. Abhayapala and A. Gupta, "Higher order differential-integral microphone arrays," *Journal of the Acoustical Society of America*, vol. 127, no. 5, pp. EL227 – EL233, April 2010. https://doi.org/10.1121/1.3402341

[58] J. Benesty and J. Chen, *Study and Design of Differential Microphone Arrays*, 1st ed. Heidelberg, Germany: Springer Verlag, 2013. https://doi.org/10.1007/978-3-642-33753-6

[59] C. Pan, J. Benesty, and J. Chen, "Design of robust differential microphone arrays with orthogonal polynomials," *Journal of the Acoustical Society of America*, vol. 138, no. 2, pp. 1079 – 1089, August 2015. https://doi.org/10.1121/1.4927690

[60] J. Benesty, J. Chen, and C. Pan, *Fundamentals of Differential Beamforming*. Springer Verlag, 2016. https://doi.org/10.1007/978-981-10-1046-0

[61] L. Wang and J. Zhu, "Flexible Beampattern Design Algorithm for Spherical Microphone Arrays," *IEEE Access*, vol. 7, pp. 139 488 – 139 498, September 2019. https://doi.org/10.1109/ACCESS.2019.2943615

[62] G. W. Elko, "Microphone array systems for hands-free telecommunication," *Speech Communication*, vol. 20, no. 3, pp. 229 – 240, 1996. https://doi.org/10.1016/S0167-6393(96)00057-X

[63] ——, "Differential Microphone Arrays," in *Audio Signal Processing for Next-Generation Multimedia Communication Systems*, Y. A. Huang and J. Benesty, Eds. Kluwer Academic Publishers, 2004, pp. 11 – 65. https://doi.org/10.1007/1-4020-7769-6_2

[64] T. Carpentier, "Spherical beampatterns with fractional orders," in *Proc. of the Forum Acusticum, 10th Convention of the European Acoustics Association (EAA)*, Torino, Italy, September 2023.

[65] C. Hold, A. Politis, L. McCormack, and V. Pulkki, "Spatial filter bank design in the spherical harmonic domain," in *Proc. of the European Signal Processing Conference (EUSIPCO)*, Dublin, Ireland, August 2021. https://doi.org/10.23919/EUSIPCO54536.2021.9616091

[66] A. Bernardini, M. D'Aria, R. Sannino, and A. Sarti, "Efficient Continuous Beam Steering for Planar Arrays of Differential Microphones," *IEEE Signal Processing Letters*, vol. 24, no. 6, pp. 794 – 798, 2017. https://doi.org/10.1109/LSP.2017.2695082

[67] G. Huang, J. Chen, and J. Benesty, "Design of Planar Differential Microphone Arrays With Fractional Orders," *IEEE/ACM Transactions on Audio, Speech, and Language Processing*, vol. 28, pp. 116 – 130, October 2019. https://doi.org/10.1109/TASLP.2019.2949219

[68] ——, "A flexible high directivity beamformer with spherical microphone arrays," *Journal of the Acoustical Society of America*, vol. 143, no. 5, pp. 3024 – 3035, May 2018. https://doi.org/10.1121/1.5038275

[69] T. Carpentier, "Spat: a comprehensive toolbox for sound spatialization in Max," *Ideas Sónicas*, vol. 13, no. 24, pp. 12 – 23, June 2021. https://hal.science/hal-03356292

[70] S. H. Linkwitz, "Active Crossover Networks for Noncoincident Drivers," *Journal of the Audio Engineering Society*, vol. 24, no. 1, pp. 2 – 8, February 1976. http://www.aes.org/e-lib/browse.cfm?elib=2649

[71] J. Meyer, *Acoustics and the Performance of Music – Manual for Acousticians, Audio Engineers, Musicians, Architects and Musical Instruments Makers*, 5th ed. Springer, 2009. https://doi.org/10.1007/978-0-387-09517-2

[72] J. Pätynen and T. Lokki, "Directivities of Symphony Orchestra Instruments," *Acta Acustica united with Acustica*, vol. 96, pp. 138 – 167, 2010. https://doi.org/10.3813/AAA.918265

[73] T. Carpentier and A. Einbond, "Spherical correlation as a similarity measure for 3-D radiation patterns of musical instruments," *Acta Acustica*, vol. 7, no. 40, pp. 1 – 16, August 2023. https://doi.org/10.1051/aacus/2023033

[74] ——, "Spherical correlation as a similarity measure for 3D radiation patterns of musical instruments," in *Proc. of the 16th Congrès Français d'Acoustique (CFA)*, Marseille, France, April 2022, pp. 1 – 6. https://hal.science/hal-03649913

[75] M. Wright, "Open Sound Control: an enabling technology for musical networking," *Organised Sound*, vol. 10, no. 3, pp. 193 – 200, December 2005. https://doi.org/10.1017/S1355771805000932